Comparative Analysis of NBC 105:1994, NBC 105:2020 and IS 1893:2002 Seismic Codes with G+8 RC Building

Er. Jeevan Gwaccha[1], Aakash Pokharel [2], Abhishek Khatri [2] and Farhan Ansari [2,*]

[1]Kathford International College of Engineering and Management, Tribhuvan University, Balkumari, Nepal
[2]Kathford International College of Engineering and Management, Tribhuvan University, Balkumari, Nepal
Email: jeevangwaccha@kathford.edu.np (J.G.); Akaspokharel@gmail.com (A.P.); aabhishekleo@gmail.com (A.K.); farhan.ansari.72445@gmail.com (F.A.)

[*]Corresponding author

***Abstract*—The Design and Construction of Buildings are done according to the prevalent codes of the locality. As the society evolve, so does the codes. In Nepal, the transition from the use of IS codes to the use of NBC has eased the sector of building construction. Although these codes to some extents are similar, greater portion of these codes remain distinct. This paper intends to differentiate between these codes with clarity. The differences in design and analysis between NBC 105:1994 ,NBC 105:2020 and IS 1893:2002, as considered by ETABS Ultimate 21.0.0 software, is presented in this article comparing the design results of parameters story displacement, story drift ratio, base shear, story shear, floor acceleration, overturning moment, torsional irregularity, moment diagrams and shear diagrams under the application of seismic load for the soil type found in Kathmandu Valley region as per the distinct code provision. From the comparison results, it shows that the IS 1893:2002 and NBC 105:1994 show almost similar results for base shear, story displacement, story drift ratio, story shear, overturning moment, floor acceleration due to the similarity in their derivation and assumption. But the results obtained from NBC 105:2020 is majorly different, the variation of results obtained from this code is more than 2 times than that of the IS 1893:2002 and NBC 105:1994 for all design parameters.**

***Keywords*—building codes, NBC 105:1994, NBC 105:2020, IS 1893:2002, ETABS, seismic provisions, RC frame, G+8 RC frame**

I. Introduction

Earthquakes are violent shaking of the ground due to the forces released during tectonic plate movement. Indian subcontinent, especially the Himalayan region, is highly prone to deadly earthquakes due to the subduction of the Indian plate underneath the Eurasian plate at the rate of approx. 4cm/year [1, 2]. The recorded history shows the level of destruction that can occur in this region repeatedly. This is one of the reasons for the necessity of a well-researched set of rules and codes for the construction of structures. Any structure should be constructed such that it has the potential to withstand its inertial forces during an earthquake which can vary according to the mass of the building itself [3]. This is the reason for the need of building codes for each region.

Building codes are prepared for a specific region with data that relate the physical and topographical characteristics of that area. Beyond the area for which the codes have been prepared, it renders less useful or sometimes useless. Thus, most regions in the world have their own building codes. In the context of Nepal, until 1994, we used to rely upon the Indian, British, or American code.

The preparation of the 1994 code introduced a new era of building construction in Nepal. After all the progress made, the use of IS code is still prevalent [4, 5]. Despite the use of these codes, the engineers as well as the clients do not have a clear insight on the differences between NBC and IS codes. It is essential that the client as well as the engineer understand the variation so that an informed decision can be made with regards to the choice between the codes. The level of variation produced using different codes on a same building can settle the uncertainty.

II. Objective of This Paper

To understand the seismic analysis procedure involved in NBC 105:1994, NBC 105:2020 and IS 1893:2002.

To study the behavior of G+8 RC building for different parameters like displacement, base shear, story drift ratio, story acceleration, story shear, torsional demand, overturning moment, moment diagram and shear diagram for a specific soil type considered for Kathmandu Valley as considered in NBC and IS code.

To compare the analysis results of G+8 RC building according to NBC and IS codes.

III. Literature Review

Each building code is based on its own set of principles, making it unwise to combine the requirements of different codes. The Indian seismic code is based on deterministic seismic hazard analysis derived from

Manuscript received June 15, 2024; revised July 1, 2024; accepted July 18, 2024; accepted September 25, 2024.

historical earthquake data, while the Nepali seismic code is based on probabilistic seismic hazard analysis of all faults within a 150 km radius of Nepal [6]. A comparative analysis has been performed by independently applying each code and then comparing the final design results.

The response spectrum provided in IS 1893 (Part I): 2002 is used for this study. This code does not specify the damping ratio for masonry structures and hence, it is assumed to be 5 percent of the critical [7, 8].

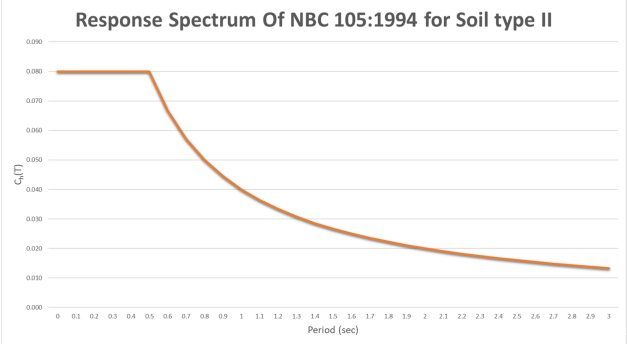

Fig. 1. Response Spectrum Curve according to NBC 105:1994 for Soil Type II.

For the seismic analysis, all three of the codes have their own response spectrum curves for different soil types as seen in the Figs. 1, 2 and 3. The spectral acceleration coefficient (Sa/g) for IS 1893:2002, basic seismic coefficient (C) for NBC 105:1994 and spectral shape factor (Ch(T)) for NBC 105:2020. The classification of sol type consideration for the IS 1893:2002 and NBC 105:1994 are similar but for the NBC 105:2020 it is entirely different consideration so to circumvent this dilemma the soil type found in Kathmandu Valley as well as the one considered as per the code practice for this location as per the codes is considered.

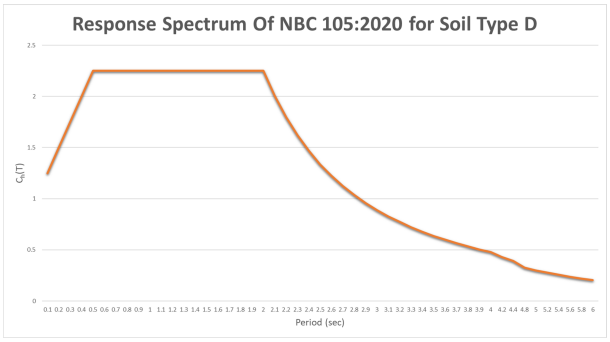

Fig. 2. Response Spectrum Curve according to NBC 105:2020 for Soil Type D.

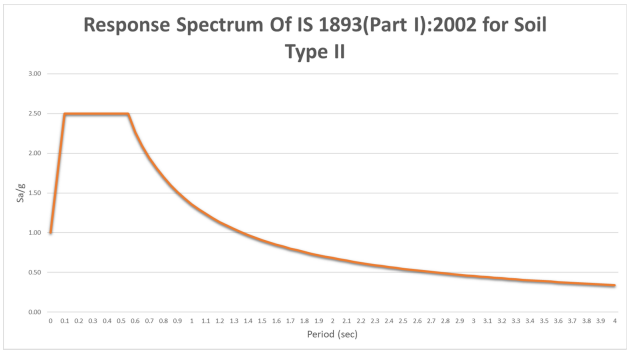

Fig. 3. Response Spectrum Curve according to IS 1893(Part I):2002 for Soil Type II.

The design parameters required for calculating design horizontal acceleration, base shear, overturning moment of RC frame structure as per NBC 105:1994, NBC 105:2020 and IS 1893:2002 is represented in Table I.

TABLE I. DESIGN PARAMETERS REQUIRED FOR SEISMIC ANALYSIS OF NBC 105:1994, NBC 105:2020 AND IS 1893:2002

Design Parameters	**NBC 105:1994**	**NBC 105:2020**	**IS 1893:2002**
Seismic Coefficient (C), ($C_h(T)$), (S_a/g)	(C) = As per Fig. 1	($C_h(T)$) = As per Fig. 2	(Sa/g) = As per Fig. 3
Time Period (T)	$T = 0.09*h/\sqrt{d}$	$T = 0.075*h^{3/4}$	$T = 0.09*h/\sqrt{d}$
Zone Factor (Z)	Z = 1	Z = 0.35	Z = 0.36
Importance Factor (I)	I = 1	I = 1	I = 1
Factor Coefficient (K), (R), (R_μ), (Ω_μ)	K = 1	K = 1.2065 $R_\mu = 4$ $\Omega_\mu = 1.5$	R = 5
Design Hz. Seismic Coefficient (C_d), ($C_d(T)$), (A_h)	$C_d = ZIK$	$C(T) = C_h(T)*Z*I$ $C_d(T) = C(T)/(R_\mu*\Omega_\mu)$	$A_h = (S_a/g)*(I/R)*(Z/2)$
Design Base Shear (V), (V_b)	$V = C_d*W_i$	$V = C_d(T)*W_i$	$V_B = A_h*W_i$

Note:
h: Total height of the building structure
d: Overall length of the building at the base in the direction under consideration (m). Or, Base dimension of the building, in meters, in the direction in which the seismic force is considered.
W_i: Seismic weight of floor *i*

According to IS 1893:2002, NBC 105:1994 and NBC 105:2020, both India and Nepal are categorized into four seismic zones, with Nepal being classified as zone V using India's zone factor. The NBC code has a higher importance factor than the IS code. NBC 105:1994 assigns an importance factor of 1 for normal residential buildings, 1.5 for public buildings, and 2 for critical structures like those supporting acid, toxic, or petroleum facilities. Meanwhile, IS 1893:2002 specifies an importance factor of 1 for normal residential buildings, 1.2 for commercial buildings with occupancy over 200, and 1.5 for important and public buildings. And NBC 105:2020 specifies an importance factor of 1 for ordinary structures (not falling in importance class I), 1.25 for those falling in importance class II (structures like schools, colleges, cinemas, assembly buildings, etc.), and

1.5 for structures of importance class III (Hospitals, fire stations, police headquarters, power stations, etc.).

The performance factor (K) and the response reduction factor (R) are based on the building's performance characteristics. Non-ductile structures, such as masonry buildings, have a higher performance factor (K) and a lower response reduction factor (R). Therefore, buildings with a lower capacity to resist lateral loads will have an increased design horizontal seismic coefficient in both codes. Both NBC and IS calculate the base shear (VB) by multiplying the design horizontal seismic coefficient by the seismic weight of the building, which includes the total dead load and a relevant percentage of the live load.

According to NBC 105:1994, the design lateral force is determined by:

$$F_i = V \times (W_i h_i)/(\Sigma W_i h_i) \quad (1)$$

where,

$F_i \rightarrow$ horizontal seismic force applied at a level designated as i.

$W_i \rightarrow$ proportion of total of gravity loads above the level of lateral restraint, contributed by level i.

$h_i \rightarrow$ height to the level designated as i from the level of lateral restraint.

$V \rightarrow$ total horizontal seismic base shear.

According to NBC 105:2020, the design lateral load is determined by:

$$F_i = V \times (W_i h_i^k)/(\Sigma W_i h_i^k) \quad (2)$$

where,

$F_i \rightarrow$ Lateral force acting at level i.

$W_i \rightarrow$ seismic weight of the structure assigned to level 'i'.

$h_i \rightarrow$ height (m) from the base to level 'i'.

$k \rightarrow$ an exponent related to the structural period as follows:

- for structure having time period $T \leq 0.5$sec, $k=1$
- for structure having time period $T \geq 2.5$sec, $k=2$
- for structure having period between 0.5 sec and 2.5 sec, k shall be determined by linear interpolation between 1 and 2.

$V \rightarrow$ horizontal seismic base shear calculated as per clause 6.2

According to IS 1893:2002, the design lateral load at each floor (i) is determined by:

$$Q_i = V_B \times (W_i h_i^2)/([\Sigma(j=1) \text{ ^}n] (W_i h_i^2)) \quad (3)$$

where,

$Q_i \rightarrow$ design lateral force at floor i.

$W_i \rightarrow$ seismic weight of floor i.

$h_i \rightarrow$ height of floor i measured from base.

$V_B \rightarrow$ Design seismic base shear.

$n \rightarrow$ Number of stories in the building is the number of levels at which the masses are located.

The load case considered for the analysis of the RC frame building according to IS 1893:2002, NBC 105:1994 and NBC 105:2020 was carried for only the earthquake loads for the design parameters like base shear, story displacement, story shear, story drift, overturning moment, shear diagram, moment diagram, and torsional irregularity. Meanwhile, the response spectrum method was considered for the story acceleration design parameter.

IV. Methodology

In this study, G+8 RC frame buildings are examined in accordance with NBC 105:1994, NBC 105:2020, and IS 1893:2002 using both the seismic coefficient method and the response spectrum method. The building is symmetric and free from configuration irregularities. The design includes a plan with 3-bays of 5 meters center-to-center in the X-direction and 4-bays of 4 meters center-to-center in the Y-direction. The building is situated in the Kathmandu Valley, with a factor (Z) specified by the NBC codes and a zone factor of V as per IS regulations. Table II shows the general building characteristics of the building used in modeling.

TABLE II. General Characteristics of Building

Building Parameters	Values
No. of Story	G+8
Total Story Height	28m
Typical Floor Height	3.5m
No. of Columns	20
Height to Width ratio of building	1.4
Length to Width ratio of building	0.75
Column Size, Concrete	400 × 400 mm, M20
Beam Size, Concrete	350 × 230 mm, M20
Slab Size, Concrete	125 mm, M20
Loads	Live Loads: 3 kN/m^2 Floor Finishes: 1 kN/m^2
Importance Factor (I)	1
Type of Building	SMRF
Soil Type Consideration	II (NBC 105:1994, IS 1893:2002), D (NBC105:2020)
Natural time Period (t)	0.65 sec

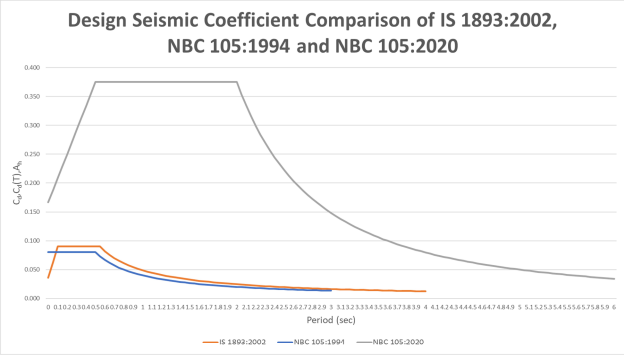

Fig. 4. Comparison of Design Seismic Coefficient According to NBC 105:1994, NBC 105:2020 and IS 1893:2002.

Fig. 4 illustrates the comparison of the design seismic coefficient (C_d, $C_d(T)$, A_h) for a SMRF frame with an importance factor of 1 and the natural period of the structure (T) used for response spectrum analysis in ETABS. It can be seen that the response spectrum of NBC 105:1994 and IS 1893:2002 is almost similar but that of NBC 105:2020 is extremely large in comparison

to both the NBC 105:1994 and IS 1893:2002 in the initial stages throughout the entirety till the end.

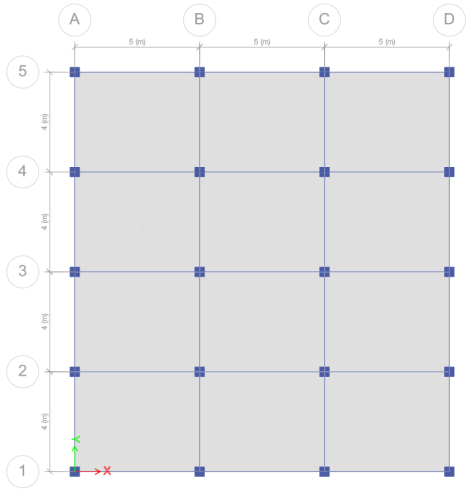

Fig. 5. Plan of RC Building.

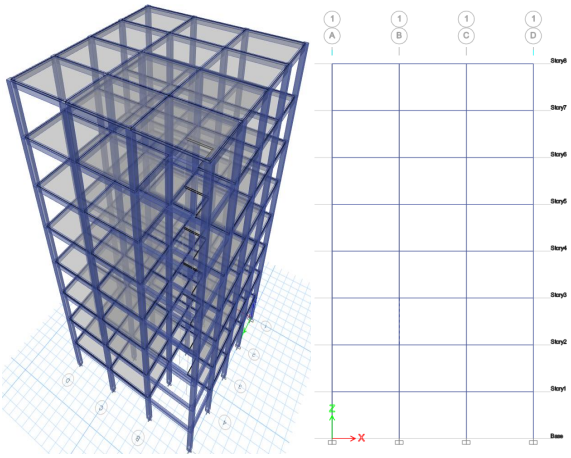

Fig. 6. 3D view of RC Building (Left), Elevation of RC Building (Right).

V. Result and Discussion

Legend	
NBC1994	NBC 105:1994 [9]
NBC2077	NBC 105:2020 [10]
IS2002	IS 1893(Part I):2002 [11]

The results for the design parameters obtained as per the codes are elaborated below:

A. Base Shear

According to Seismic Coefficient Method for a specific soil type of Kathmandu Valley, the base shear data obtained for the model is observed as in the Table III and graphically as in Fig. 7.

As can be seen in the Table III, the base shear of the three codes has the same values for base shear in their respective three modes. And it can be observed thar the base shear due of NBC 105:2020 is **more than twice** than that of either the base shear obtained from NBC 105:1994 and from IS 1893:2002. Whereas, the base shear difference of NBC 105:1994 is slightly higher than that of IS 1893:2002.

If we assume that the base shear of NBC 105:2020 as the maximum (100%) value then, the base shear of NBC 105:1994 is about 41.768%, the base shear of IS 1893:2002 is about 40.877% in comparison to the NBC 105:2020.

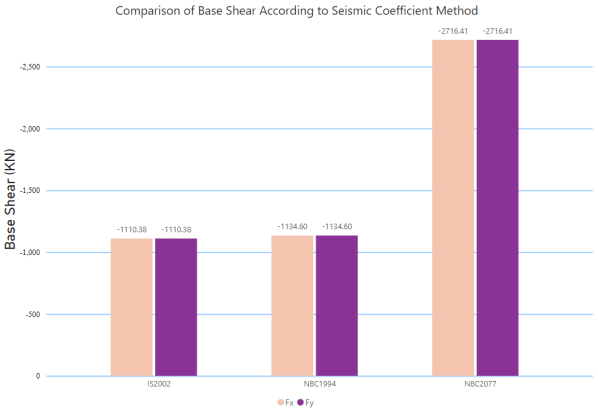

Fig. 7. Comparison of Base Shear (kN) According to Seismic Coefficient Method of NBC 105:1994, NBC 105:2020 and IS 1893:2002.

TABLE III. Results Obtained for Story Shear as per NBC 105:1994, NBC 105:2020 and IS 1893:2002 According to Seismic Coefficient Method

Base Shear (KN)				
Lateral Load		**NBC 105:1994**	**NBC 105:2020**	**IS 1893:2002**
EQ_X	Mode 1	-1134.60	-1110.38	-2716.41
	Mode 2	-1134.60	-1110.38	-2716.41
	Mode 3	-1134.60	-1110.38	-2716.41
EQ_Y	Mode 1	-1134.60	-1110.38	-2716.41
	Mode 2	-1134.60	-1110.38	-2716.41
	Mode 3	-1134.60	-1110.38	-2716.41

EQ_x: Lateral earth load in X-direction
EQ_y: Lateral earth load in Y-direction

B. Floor Acceleration

According to Modal Response Spectrum Method for the specific soil type of Kathmandu Valley, the floor acceleration for each level due to the response spectrum in both the X-direction and Y-direction show their effect in the both directions as in the Figs. 8a-b through Figs. 8e-f below of the tabulated data presented in the Tables: Table IVa, Table IVb and Table IVc for their respective directional acceleration.

On observation of the Figs. 8a through 8c, it is seen that the floor acceleration achieved by the model designed as per NBC 105:1994 for the first story is the largest amongst all those for this story only, but after the first story the rest of the stories modelled as per NBC 105:2020 achieve the highest floor acceleration later maxing out at the story height of 24.0m at the U_x=27985.66mm/sec^2, followed by the acceleration of NBC 105:1994 design model at U_x=15928.62mm/sec^2, and he acceleration of IS 1893:2002 design model at U_x=5733.95mm/sec^2, as can be seen in the Table IVa and the Fig. 8a.

Similarly, the floor acceleration achieved by the model designed as per NBC 105:1994 for the first story is the largest amongst all those for this story only, but after the first story the rest of the stories modelled as per NBC 105:2020 achieve the highest floor acceleration later maxing out at the story height of 24.0m at the U_y=31121.32mm/sec^2, followed by the acceleration of NBC 105:1994 design model at U_y=16484.35mm/sec^2, and he acceleration of IS 1893:2002 design model at U_y=5933.99mm/sec^2, as can be seen in the Table IVa and the Fig. 8d.

Though there is no vertical component of the actual acceleration, but the effect of the response spectrum causes the ground motion to introduce some degree of vertical motion as can be seen form the data in the Table IV4c and the Fig. 8e and Fig. 8f.

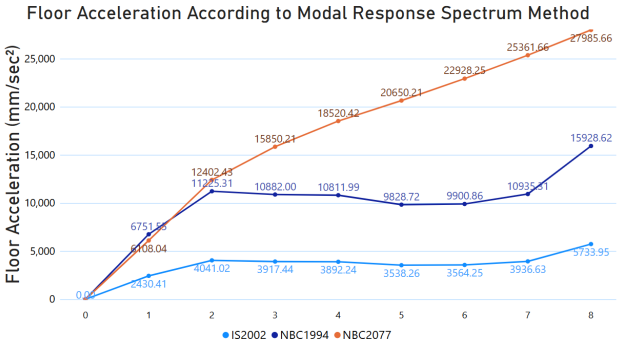

Fig. 8a. Comparison of X-directional Floor Acceleration (mm/sec2) in X-Direction According to Modal Response Spectrum Method.

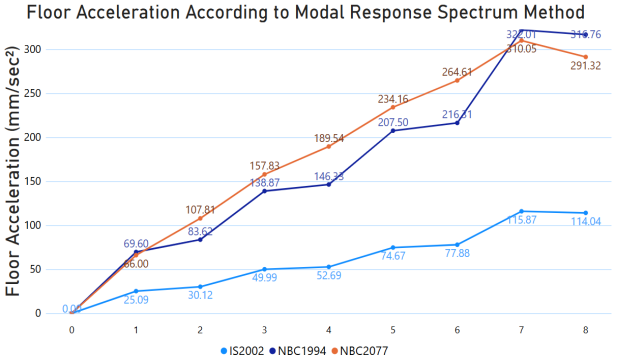

Fig. 8b. Comparison of X-directional Floor Acceleration (mm/sec^2) in Y-Direction According to Modal Response Spectrum Method.

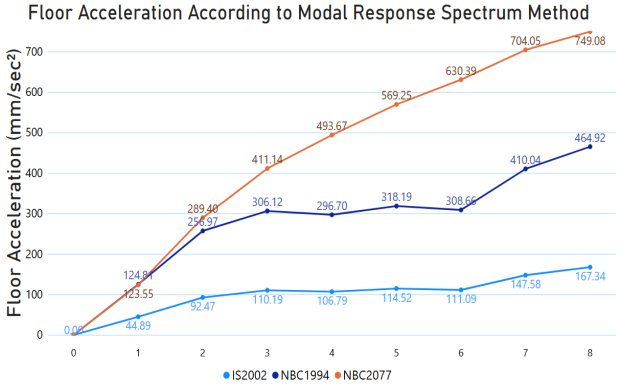

Fig. 8c. Comparison of Y-directional Floor Acceleration (mm/sec^2) in X-Direction According to Modal Response Spectrum Method.

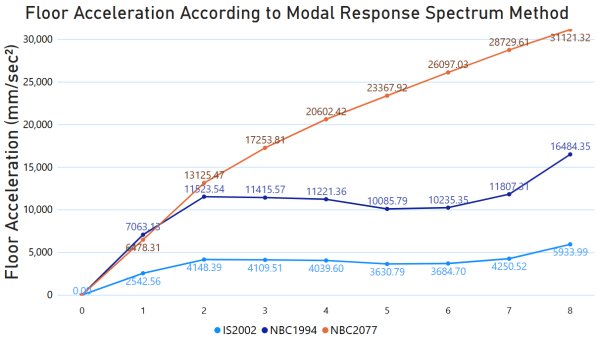

Fig. 8d. Comparison of Y-directional Floor Acceleration (mm/sec^2) in Y-Direction According to Modal Response Spectrum Method.

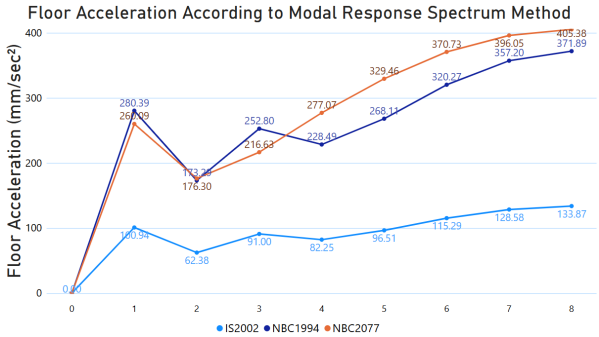

Fig. 8e. Comparison of Z-directional Floor Acceleration (mm/sec^2) in X-Direction According to Modal Response Spectrum Method.

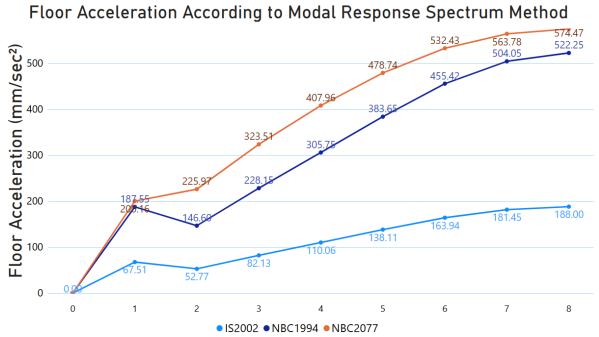

Fig. 8f. Comparison of Z-directional Floor Acceleration (mm/sec^2) in Y-Direction According to Modal Response Spectrum Method.

Lastly, it can also be seen in the Figs. 8b and Fig. 8c the direction of the floor acceleration is in perpendicular direction to the direction of response motion. This can be accounted to multiple different reasons, which are elaborated as:

- **Structural Coupling:** Buildings are three-dimensional structures, and their components are interconnected. When a force is applied in one direction, it can cause deformations and movements in other directions due to the coupling of structural elements.
- **Torsional Effects:** If the building is not perfectly symmetrical or if the mass distribution is uneven, applying a force in the Y-direction can induce torsional (rotational) motion. This torsion can cause parts of the building to move in the X-direction.
- **Accidental Eccentricity:** During an earthquake, the actual center of mass of the building may not

coincide with the assumed center of mass. This discrepancy can cause additional forces and moments, leading to motion in the X-direction even when the primary force is in the Y-direction.

- **Inertial Forces:** According to Newton's second law, the inertial forces generated by the acceleration in the Y-direction can cause secondary movements in the X-direction, especially if the building has irregularities or asymmetries.

TABLE IVA: RESULTS OBTAINED FOR FLOOR ACCELERATION AS PER NBC 105:1994, NBC 105:2020 AND IS 1893:2002 ACCORDING TO RESPONSE SPECTRUM METHOD

Floor Acceleration: U_X (mm/sec^2)				
Story		**NBC 105:1994**	**NBC 105:2020**	**IS 1893:2002**
Base	X	0	0	0
	Y	0	0	0
1	X	6751.55	6108.04	2430.41
	Y	69.6	66	25.09
2	X	11225.31	12402.43	4041.02
	Y	83.62	107.81	30.12
3	X	10882	15850.21	3917.44
	Y	138.87	157.83	49.99
4	X	10811.99	18520.42	3892.24
	Y	146.33	189.54	52.69
5	X	9828.72	20650.21	3538.26
	Y	207.5	234.16	74.67
6	X	9900.86	22928.25	3564.25
	Y	216.31	264.61	77.88
7	X	10935.31	25361.66	3936.63
	Y	322.01	310.05	115.87
8	X	15928.62	27985.66	5733.95
	Y	316.76	291.32	114.04

TABLE IVB. RESULTS OBTAINED FOR FLOOR ACCELERATION AS PER NBC 105:1994, NBC 105:2020 AND IS 1893:2002 ACCORDING TO RESPONSE SPECTRUM METHOD

Floor Acceleration: U_Y (mm/sec^2)				
Story		**NBC 105:1994**	**NBC 105:2020**	**IS 1893:2002**
Base	X	0	0	0
	Y	0	0	0
1	X	124.81	123.55	44.89
	Y	7063.13	6478.31	2542.56
2	X	256.97	289.4	92.47
	Y	11523.54	13125.47	4148.39
3	X	306.12	411.14	110.19
	Y	11415.57	17253.81	4109.51
4	X	296.7	493.67	106.79
	Y	11221.36	20602.42	4039.6
5	X	318.19	569.25	114.52
	Y	10085.79	23367.92	3630.79
6	X	308.66	630.39	111.09
	Y	10235.35	26097.03	3684.7
7	X	410.04	704.05	147.58
	Y	11807.31	28729.61	4250.52
8	X	464.92	749.08	167.34
	Y	16484.35	31121.32	5933.99

TABLE IVC. RESULTS OBTAINED FOR FLOOR ACCELERATION AS PER NBC 105:1994, NBC 105:2020 AND IS 1893:2002 ACCORDING TO RESPONSE SPECTRUM METHOD

Floor Acceleration: U_Z (mm/sec^2)				
Story		**NBC 105:1994**	**NBC 105:2020**	**IS 1893:2002**
Base	X	0	0	0
	Y	0	0	0
1	X	280.39	260.09	100.94
	Y	187.55	200.16	67.51
2	X	173.29	176.3	62.38
	Y	146.6	225.97	52.77
3	X	252.8	216.63	91
	Y	228.15	323.51	82.13
4	X	228.49	277.07	82.25
	Y	305.75	407.96	110.06
5	X	268.11	329.46	96.51
	Y	383.65	478.74	138.11
6	X	320.27	370.73	115.29
	Y	455.42	532.43	163.94
7	X	357.2	396.05	128.58
	Y	504.05	563.78	181.45
8	X	371.89	405.38	133.87
	Y	522.25	574.47	188

C. *Overturning Moment*

According to Seismic Coefficient Method for the specific soil type of Kathmandu Valley, the Overturning Moment in both the direction of the lateral load application is expressed in Table V, and the Figures for X-directional and Y-directional effect are shown in the Figs. 9a and 9b.

The negative signs for the data in the table is due to the structure experiencing the moment in the counter direction to the actual load application, that is, counter-clockwise direction. The figures, Fig. 9a and 9b are plotted using the negative values, and if we convert to the absolute values the result is the same so either comparison observed is the same result.

Considering only the absolute values then it can be seen that the moment is always the largest for the design model of NBC 105:2020 throughout the entirety of the building at each story, experiencing the same amount of moment in both the X and Y-direction. Though the moment in Y-direction aligns with the direction of the load application while the moment in X-direction is in the opposite direction to the load application.

The moment observed in NBC 105:2020 design model is almost equal to 53000 KN-m, NBC 105:1994 deign model is almost 21500KN-m and IS 1893:2002 is almost 23600KN-m. form this data, it can be observed that the result of the latest NBC 105:2020 obtains higher moment than the other two models and has to be modelled with advance technology and higher strength materials to resist this moment.

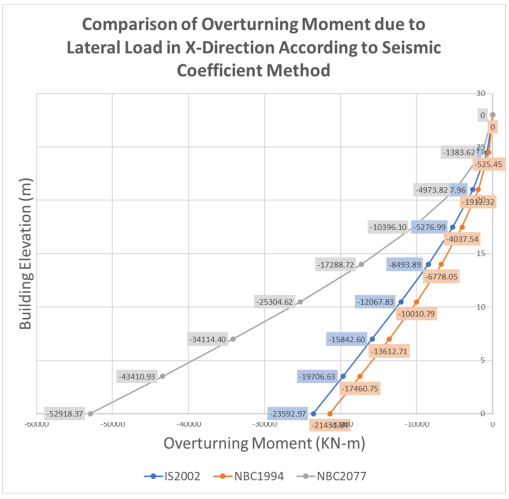

Fig. 9a. Comparison of Overturning Moment (kN-m) due to Lateral Load in X-direction According to Seismic Coefficient Method of NBC 105:1994, NBC 105:2020 and IS 1893:2002.

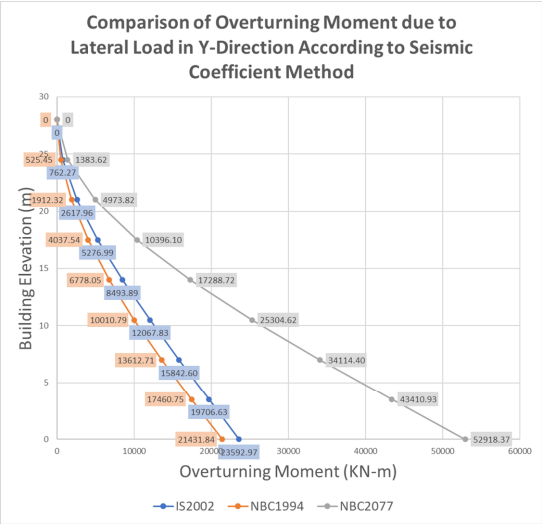

Fig. 9b. Comparison of Overturning Moment (kN-m) due to Lateral Load in Y-direction According to Seismic Coefficient Method of NBC 105:1994, NBC 105:2020 and IS 1893:2002.

TABLE V. RESULTS OBTAINED FOR OVERTURNING MOMENT AS PER NBC 105:1994, NBC 105:2020 AND IS 1893:2002 ACCORDING TO SEISMIC COEFFICIENT METHOD

		Overturning Moment (KN-m)		
Story		**NBC 105:1994**	**NBC 105:2020**	**IS 1893:2002**
Base	EQ_X	-21431.84	-52918.37	-23592.97
	EQ_Y	21431.84	52918.37	23592.97
1	EQ_X	-17460.75	-43410.93	-19706.63
	EQ_Y	17460.75	43410.93	19706.63
2	EQ_X	-13612.71	-34114.40	-15842.60
	EQ_Y	13612.71	34114.40	15842.60
3	EQ_X	-10010.79	-25304.62	-12067.83
	EQ_Y	10010.79	25304.62	12067.83
4	EQ_X	-6778.04	-17288.72	-8493.89
	EQ_Y	6778.04	17288.72	8493.89
5	EQ_X	-4037.54	-10396.10	-5276.99
	EQ_Y	4037.54	10396.10	5276.99
6	EQ_X	-1912.32	-4973.82	-2617.96
	EQ_Y	1912.32	4973.82	2617.96
7	EQ_X	-525.46	-1383.62	-762.27
	EQ_Y	525.46	1383.62	762.27
8	EQ_X	0	0	0
	EQ_Y	0	0	0

D. Story Displacement

According to Seismic Coefficient Method for the specific soil type of Kathmandu Valley, the Overturning Moment in X-direction and Y-direction of the lateral load application are expressed in tables 6a and 6b, and the figures for X-directional and Y-directional effect are shown in the Figs. 10a and 10b.

From Table VIa and Fig. 10a for the X-directional lateral loading, it is seen that the story displacement throughout each story is the highest for the NBC 105:2020 model and, that of the NBC 105:1994 and IS 1893:2002 model is close together.

On comparing the story displacement data, the displacement experienced by each story of NBC 105:220 model is almost 2.4 times than that of displacement of each corresponding story of NBC 105:1994 model with only value difference in the 1/100th decimal position throughout the building. However, the story displacement of IS 1893:2002 model ranges from the 2.4 times to 2.2 times the difference from the NBC 105:2020 model which decreases as we go to the higher stories with the decrease occurring in the 1/100th decimal value range.

Similarly, from Table VIb and Fig. 10b for the Y-directional lateral loading, it is seen that the story displacement throughout each story is the highest for the NBC 105:2020 model and, that of the NBC 105:1994 and IS 1893:2002 model is close together.

On comparing the story displacement data, the displacement experienced by each story of NBC 105:220 model is almost 2.4 times than that of displacement of each corresponding story of NBC 105:1994 model with only value difference in the 1/100th decimal position throughout the building. However, the story displacement of IS 1893:2002 model ranges from about 2.4 times to 2.2 times the difference from the NBC 105:2020 model which decreases as we go to the higher stories with the decrease occurring in the 1/100th decimal value range.

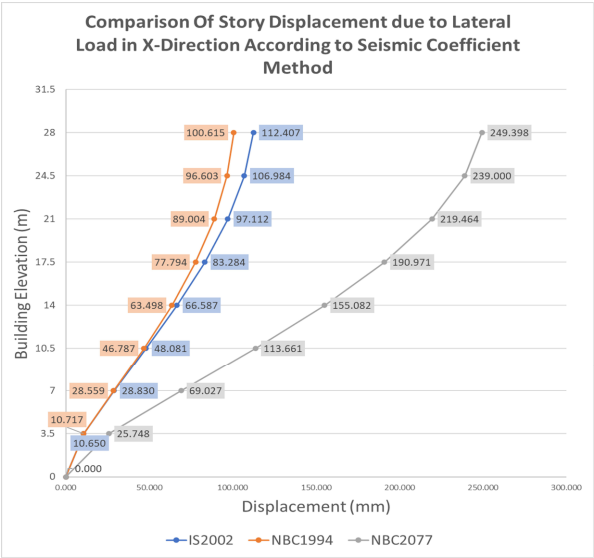

Fig. 10a. Comparison of Story Displacement (mm) due to Lateral Load in X-direction According to Seismic Coefficient Method of NBC 105:1994, NBC 105:2020 and IS 1893:2002.

TABLE VIA: RESULTS OBTAINED FOR STORY DISPLACEMENT AS PER NBC 105:1994, NBC 105:2020 AND IS 1893:2002 ACCORDING SEISMIC COEFFICIENT METHOD IN THE X-DIRECTION

		Story Displacement (mm)		
Story		**NBC 105:1994**	**NBC 105:2020**	**IS 1893:2002**
Base	EQ_X	0	0	0
	EQ_Y	0	0	0
1	EQ_X	10.72	25.75	10.65
	EQ_Y	0.04	0.08	0.01
2	EQ_X	28.56	69.03	28.83
	EQ_Y	0.06	0.09	0.08
3	EQ_X	46.79	113.66	48.08
	EQ_Y	0.05	0.13	0.17
4	EQ_X	63.50	155.08	66.59
	EQ_Y	0.08	0.28	0.28
5	EQ_X	77.79	190.97	83.28
	EQ_Y	0.14	0.46	0.39
6	EQ_X	89.00	219.46	97.11
	EQ_Y	0.21	0.66	0.51
7	EQ_X	96.60	239	106.98
	EQ_Y	0.30	0.89	0.64
8	EQ_X	100.62	249.4	112.41
	EQ_Y	0.38	1.10	0.76

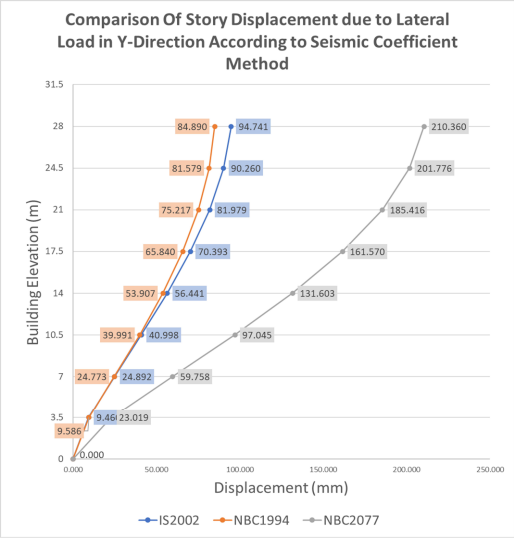

Fig. 10b. Comparison of Story Displacement (mm) due to Lateral Load in Y-direction According to Seismic Coefficient Method of NBC 105:1994, NBC 105:2020 and IS 1893:2002.

TABLE VIB: RESULTS OBTAINED FOR STORY DISPLACEMENT AS PER NBC 105:1994, NBC 105:2020 AND IS 1893:2002 ACCORDING SEISMIC COEFFICIENT METHOD IN THE Y-DIRECTION

Story		Story Displacement (mm)		
		NBC 105:1994	NBC 105:2020	IS 1893:2002
Base	EQ_X	0	0	0
	EQ_Y	0	0	0
1	EQ_X	0.02	0.02	0.04
	EQ_Y	9.59	23.02	9.46
2	EQ_X	0.07	0.21	0.17
	EQ_Y	24.77	59.76	24.89
3	EQ_X	0.17	0.49	0.33
	EQ_Y	39.99	97.04	40.99
4	EQ_X	0.28	0.80	0.51
	EQ_Y	53.91	131.60	56.44
5	EQ_X	0.40	1.11	0.69
	EQ_Y	65.84	161.57	70.39
6	EQ_X	0.53	1.44	0.87
	EQ_Y	75.22	185.42	81.98
7	EQ_X	0.65	1.77	1.06
	EQ_Y	81.58	201.78	90.26
8	EQ_X	0.76	2.04	1.21
	EQ_Y	84.89	210.36	94.74

E. *Story Drift Ratio*

According to Seismic Coefficient Method for the specific soil type of Kathmandu Valley, the Story Drift Ratio observed due to lateral load in X-direction and Y-direction of the lateral load application are expressed in Tables VIIa and VIIb, and the figures for X-directional and Y-directional effect are shown in the Figs. 11a and 11b.

From the Fig. 11a and Table VIIa for the X-directional lateral loading, we can see that the story drift ratio for the third story (elevation=10.5m) is the highest for the respective design coeds.

However, one is larger than the others which is of the NBC 105:2020 model with the story drift ratio of 1.28E-2 (where **E-2 is the exponent with the power -2**; 1.28E-2 = 1.28×10^{-2}) while the story drift ratio of the NBC 105:1994 model is 5.21E-3 and the story drift of IS 1893:2002 is 5.50E-3.

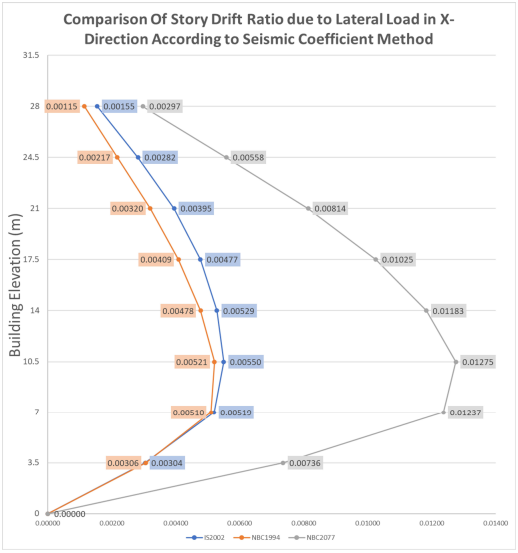

Fig. 11a. Comparison of Story Drift due to Lateral Load in X-direction According to Seismic Coefficient Method of NBC 105:1994, NBC 105:2020 and IS 1893:2002.

TABLE VIIA: RESULTS OBTAINED FOR STORY DRIFT RATIO AS PER NBC 105:1994, NBC 105:2020 AND IS 1893:2002 ACCORDING TO SEISMIC COEFFICIENT METHOD IN THE X-DIRECTION

Story		Story Drift Ratio		
		NBC 105:1994	NBC 105:2020	IS 1893:2002
Base	EQ_X	0	0	0
	EQ_Y	0	0	0
1	EQ_X	3.06E-03	7.36E-03	3.04E-03
	EQ_Y	1.10E-05	2.30E-05	2.00E-06
2	EQ_X	5.10E-03	1.24E-02	5.19E-03
	EQ_Y	5.00E-06	1.70E-05	2.00E-05
3	EQ_X	5.21E-03	1.28E-02	5.50E-03
	EQ_Y	1.10E-05	3.40E-05	2.70E-05
4	EQ_X	4.78E-03	1.18E-02	5.29E-03
	EQ_Y	1.50E-05	4.20E-05	3.00E-05
5	EQ_X	4.09E-03	1.03E-02	4.77E-03
	EQ_Y	1.80E-05	4.90E-05	3.20E-05
6	EQ_X	3.20E-03	8.14E-03	3.95E-03
	EQ_Y	2.10E-05	5.80E-05	3.50E-05
7	EQ_X	2.17E-03	5.58E-03	2.82E-03
	EQ_Y	2.50E-05	6.60E-05	3.80E-05
8	EQ_X	1.15E-03	2.97E-03	1.55E-03
	EQ_Y	2.30E-05	6.00E-05	3.40E-05

TABLE VIIB: RESULTS OBTAINED FOR STORY DRIFT RATIO AS PER NBC 105:1994, NBC 105:2020 AND IS 1893:2002 ACCORDING TO SEISMIC COEFFICIENT METHOD IN THE Y-DIRECTION

Story		Story Drift Ratio		
		NBC 105:1994	NBC 105:2020	IS 1893:2002
Base	EQ_X	0	0	0
	EQ_Y	0	0	0
1	EQ_X	5.00E-06	6.00E-06	1.00E-05
	EQ_Y	2.74E-03	6.58E-03	2.70E-03
2	EQ_X	2.00E-05	5.60E-05	3.70E-05
	EQ_Y	4.34E-03	1.05E-02	4.41E-03
3	EQ_X	2.90E-05	8.00E-05	4.80E-05
	EQ_Y	4.36E-03	1.07E-02	4.60E-03
4	EQ_X	3.30E-05	8.70E-05	5.10E-05
	EQ_Y	3.98E-03	9.87E-03	4.41E-03
5	EQ_X	3.40E-05	9.10E-05	5.10E-05
	EQ_Y	3.41E-03	8.56E-03	3.99E-03
6	EQ_X	3.50E-05	9.30E-05	5.20E-05
	EQ_Y	2.68E-03	6.81E-03	3.31E-03
7	EQ_X	3.60E-05	9.40E-05	5.20E-05
	EQ_Y	1.82E-03	4.67E-03	2.37E-03
8	EQ_X	3.00E-05	7.80E-05	4.30E-05
	EQ_Y	9.46E-04	2.45E-03	1.28E-03

Similarly, from the Fig. 11b and Table VIIb for the Y-directional lateral loading, we can see that the story drift ratio for the third story (elevation = 10.5m) is the highest for the respective design coeds.

However, one is larger than the others which is of the NBC 105:2020 model with the story drift ratio of 1.28E-2 (where **E-2 is the exponent with the power -2**; 1.28E-2 = 1.28×10^{-2}) while the story drift ratio of the NBC 105:1994 model is 5.21E-3 and the story drift of IS 1893:2002 is 5.50E-3.

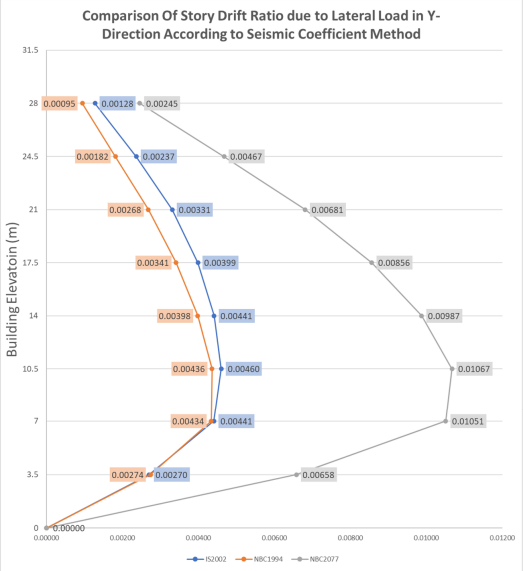

Fig. 11b. Comparison of Story Drift due to Lateral Load in Y-direction According to Seismic Coefficient Method of NBC 105:1994, NBC 105:2020 and IS 1893:2002.

F. *Story Shear*

According to Seismic Coefficient Method for the specific soil type of Kathmandu Valley, the Story Shear observed due to lateral load in X-direction and Y-direction of the lateral load application are expressed in Tables VIIIa and 8b, and the figures for X-directional and Y-directional effect are shown in the Figs. 12a and 12b.

TABLE VIIIA: RESULTS OBTAINED FOR STORY SHEAR AS PER NBC 105:1994, NBC 105:2020 AND IS 1893:2002 ACCORDING TO SEISMIC COEFFICIENT METHOD IN THE X-DIRECTION

Story		Story Shear (KN) NBC 105:1994	NBC 105:2020	IS 1893:2002
Base	EQ_X	0	0	0
	EQ_Y	0	0	0
1	EQ_X	-1134.60	-2716.41	-1110.38
	EQ_Y	0	0	0
2	EQ_X	-1099.44	-2656.15	-1104.01
	EQ_Y	0	0	0
3	EQ_X	-1029.12	-2517.08	-1078.51
	EQ_Y	0	0	0
4	EQ_X	-923.64	-2290.26	-1021.13
	EQ_Y	0	0	0
5	EQ_X	-783.00	-1969.32	-919.11
	EQ_Y	0	0	0
6	EQ_X	-607.20	-1549.22	-759.72
	EQ_Y	0	0	0
7	EQ_X	-396.25	-1025.77	-530.20
	EQ_Y	0	0	0
8	EQ_X	-150.13	-395.32	-217.79
	EQ_Y	0	0	0

TABLE VIIIB: RESULTS OBTAINED FOR STORY SHEAR AS PER NBC 105:1994, NBC 105:2020 AND IS 1893:2002 ACCORDING TO SEISMIC COEFFICIENT METHOD IN THE Y-DIRECTION

Story		Story Shear (KN) NBC 105:1994	NBC 105:2020	IS 1893:2002
Base	EQ_X	0	0	0
	EQ_Y	0	0	0
1	EQ_X	0	0	0
	EQ_Y	-1134.60	-2716.41	-1110.38
2	EQ_X	0	0	0
	EQ_Y	-1099.44	-2656.15	-1104.01
3	EQ_X	0	0	0
	EQ_Y	-1029.12	-2517.08	-1078.51
4	EQ_X	0	0	0
	EQ_Y	-923.64	-2290.26	-1021.13
5	EQ_X	0	0	0
	EQ_Y	-783.00	-1969.32	-919.11
6	EQ_X	0	0	0
	EQ_Y	-607.20	-1549.22	-759.72
7	EQ_X	0	0	0
	EQ_Y	-396.25	-1025.77	-530.20
8	EQ_X	0	0	0
	EQ_Y	-150.13	-395.32	-217.79

From the Figs. 12a and 12b and, Table VIIIa and 8b for the X-directional and Y-directional lateral loading, we can see that the base story experiences the maximum amount of story shear equaling to about 2716.41KN for the NBC 105:2020 model while that of the NBC 105:1994 model is 1134.60KN and for IS 1893:2002 model is 1110.38KN for the respective directional lateral loading, the negative sign to value is to show that the value in the opposite direction to the load application.

The largest amount of story shear is experienced by the NBC 105:2020 model then by the NBC 105:1994 model and the least in comparison by the IS 1893:2002 model for both the X-directional and Y-directional lateral loading.

However, it can also be seen from the table that the story shear for the IS 1893:2002 model is the higher value from the highest story in comparison to the NBC 105:1994 model but as we progress to the lower stories the story shear of the IS 1893:2002 model max.'s out at 1110.38KN while that of NBC 105:1994 max.'s out at 1134.60KN for both the X-directional and Y-directional lateral loading.

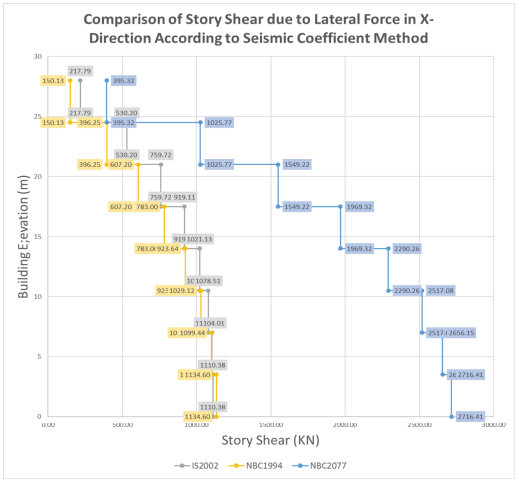

Fig. 12a. Comparison of Story Shear (kN) due to Lateral Load in X-direction According to Seismic Coefficient Method of NBC 105:1994, NBC 105:2020 and IS 1893:2002.

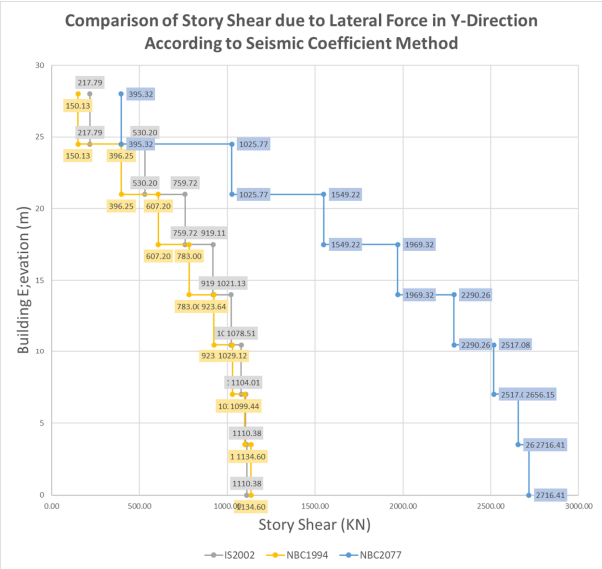

Fig. 12b. Comparison of Story Shear (kN) due to Lateral Load in Y-direction According to Seismic Coefficient Method of NBC 105:1994, NBC 105:2020 and IS 1893:2002

G. *Torsional Irregularity*

According to the IS 1893:2002 and NBC 105:2020 there is provision for the check of Torsional Irregularity but the same can't be said for NBC 105:1994 as it lacks mention of any statement related to torsional irregularity. Hence, the NBC 105:1994 is not feasible for its application of a building experiencing torsion.

According to IS 1893:2002, the torsional irregularity is considered to exist when the maximum story drift is more than 1.2 time the average story drift of the building as shown in Table IV [11].

TABLE IX. TORSIONAL IRREGULARITY AS STATED IN IS 1893:2002

Directional Lateral Load	1.2×Average Story Drift	Max. Story Drift	Torsional Irregularity
EQ_X	0.0107	0.0128	Exists
EQ_Y	0.00406	0.0046	Exists

According to NBC 105:2020, there is existence of torsional irregularity in the building structure if the maximum horizontal story displacement in the direction motion due to lateral load is more than 1.5 time the minimum horizontal displacement in the same direction as shown in Table V.

TABLE X. TORSIONAL IRREGULARITY AS STATED IN IS 1893:2002

Directional Lateral Load	1.5*Min. Story Displacement (mm)	Max. Story Displacement (mm)	Torsional Irregularity
EQ_X	38.622	249.398	Exists
EQ_Y	34.528	210.36	Exists

H. *Moment Diagram and Shear Diagram*

The Figs. 13a and 13b are the moment and shear diagrams of IS 1893:2002 design model about the grid 1 of the design model about the X-directional and Y-directional lateral loading respectively.

The red regions of the elements shown in the diagram depict that those models are close their capacity limit and are experiencing higher stain be it in shear or moment. And, the elements showing yellow region in the stress diagram depict that those elements are experiencing moderate amount of stress in shear and moment in their respective diagrams.

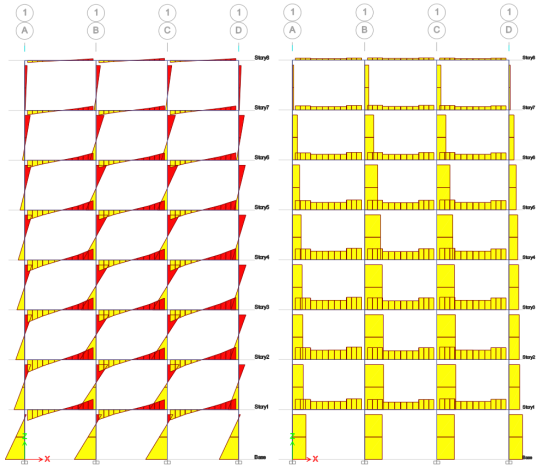

Fig. 13a. Moment Diagram (Left) and Shear Diagram (Right) due to lateral Load in X-Direction Along Grid 1 of IS 1893:2002.

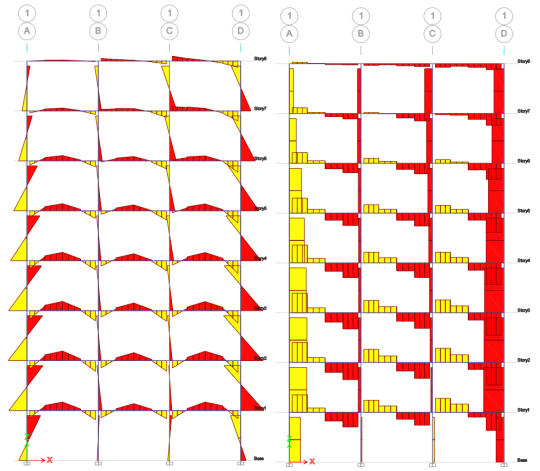

Fig. 13b. Moment Diagram (Left) and Shear Diagram (Right) due to lateral Load in Y-Direction Along Grid 1 of IS 1893:2002.

The Figs. 14a and 14b are the moment and shear diagrams of NBC 105:2020 design model about the grid 1 of the design model about the X-directional and Y-directional lateral loading respectively.

The red regions of the elements shown in the diagram depict that those models are close their capacity limit and are experiencing higher stain be it in shear or moment. And, the elements showing yellow region in the stress diagram depict that those elements are experiencing moderate amount of stress in shear and moment in their respective diagrams.

The Figs. 15a and 15b are the moment and shear diagrams of NBC 105:1994 design model about the grid 1 of the design model about the X-directional and Y-directional lateral loading respectively.

The red regions of the elements shown in the diagram depict that those models are close their capacity limit and are experiencing higher stain be it in shear or moment. And, the elements showing yellow region in the stress diagram depict that those elements are experiencing moderate amount of stress in shear and moment in their respective diagrams.

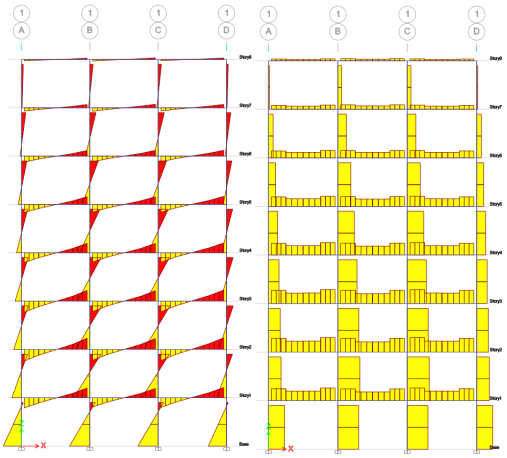

Fig. 14a. Moment Diagram (Left) and Shear Diagram (Right) due to lateral Load in X-Direction Along Grid 1 of NBC 105:2020.

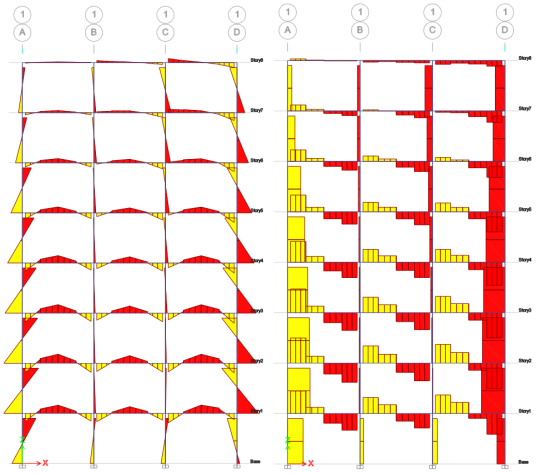

Fig. 14b. Moment Diagram (Left) and Shear Diagram (Right) due to lateral Load in Y-Direction Along Grid 1 of NBC 105:2020.

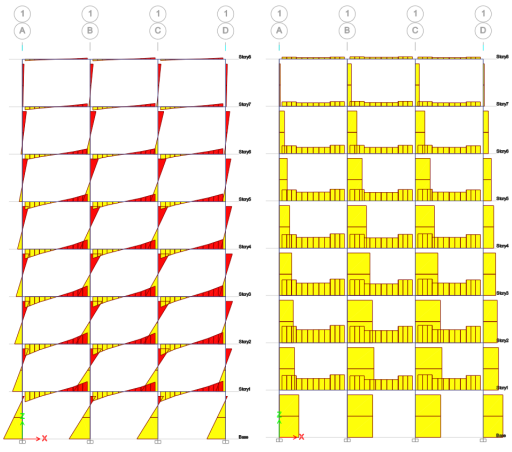

Fig. 15a. Moment Diagram (Left) and Shear Diagram (Right) due to lateral Load in X-Direction Along Grid 1 of NBC 105:1994.

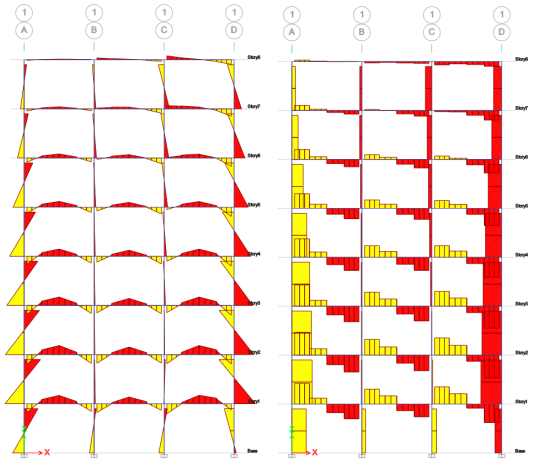

Fig. 15b. Moment Diagram (Left) and Shear Diagram (Right) due to lateral Load in Y-Direction Along Grid 1 of NBC 105:1994.

VI. Conclusion

From the comparative analysis of the G+8 RC building for the different codes at location of specific soil category of NBC 105:1994, NBC 105:2020 and IS 1893:2002, the following conclusions are drawn:

- For all three-building code application, NBC 105:2020 shows higher values for all the design parameters in comparison to the other two codes NBC 105:1994 and IS 1893:2002. This is due to the seismic coefficient, for the NBC 105:1994 and IS 1893:2002 is almost similar in value but that of NBC 105:2020 is very distinct and large thus resulting larger outcomes hence requiring similarly more adept and through design to withstand the resulting heavier strains.
- Though in some cases, Story Shear and Story Drift Ratio, the IS 1893:2002 shows higher strain initially in comparison to NBC 105:1994 model results but due to the IS 1893:2002 code reaching its maximum strain at the lower strain than that of the NBC 105:1994 the design requirement of the NBC 105:1994 is slightly higher in comparison. While in the other cases, the resulting data is mostly always larger than the data obtained from NBC 105:1994.
- Torsional demand can't be met for the building designed as per the NBC 105:1994 code since it lacks any provision for the design of building for torsion.
- The building designed on NBC 105:2020 is bound to be more stressed for the same design when compared to other building codes thus introducing the requirement for redesign of the entire structure since the material selection has to be altered and the design parameters to be adjusted to achieve the safety parameter as per the design code. While the obtained results for the NBC 105:1994 and IS 1893:2002 is within the desired safety parameter hence the obtained results can be used for its further checks and construction.

- NBC 105 yields greater seismic demand and is more conservative than IS 1893.
- From the moment and shear diagrams for each of the codes, visually one can see that the elemental stress is higher for the NBC 105:2020 model elements than that of NBC 105:1994 and IS 1893:2002 model hence requiring similarly different approach and redesign of the components.

Conflict of Interest

The authors declare no conflict of interest.

Author Contributions

Er. Jeevan Gwachha provided insights on the research and was involved as the research mentor and supervisor and was responsible for the review of the progress of the paper, Mr. Aakash Pokharel was responsible for the research model setup for all the building codes and wrote the introduction and objective of this paper, Mr. Abhishek Khatri was responsible for the data and result verification and collection, and wrote literature review and methodology of this paper, Mr. Farhan Ansari was responsible for the data analysis and visualization preparation and wrote the result and discussion, and conclusion of the paper; all authors had approved the final version.

References

[1] S. Nienhuys, *Seismic Building Codes in the Himalaya Region Questions & Answers Related to the 2015 Nepal Earthquake*, 2016.
[2] P. Pandit and M. Vasudev, "Comparative analysis of NBC 105: 1994 and is 1893: 2016 seismic codes with G+21 RC building," *International Research Journal of Engineering and Technology (IRJET),* vol. 6, no. 11, p. 1995, 2019.
[3] J. Gwachha, *Study of Soft Story Response of Typical Building of NBC*, 2022.
[4] A. Shrestha, "Comparison between common seismic codes used in Nepal and Eurocode 8: Study case analysis of RC building," *České vysoké učení technické v Praze. Vypočetní a informační centrum*., 2018.
[5] P. Neupane and S. Shrestha, "Comparative analysis of seismic codes of Nepal and India for RC buildings," *International Journal of Engineering Trends and Technology,* vol. 28, no. 2, pp. 102–105, 2015.
[6] E. A. Aryal and E. S. Dhungana, "Comparative analysis of NBC with IS code for RC structures," *International Research Journal of Engineering and Technology (IRJET),* vol. 6, no. 24, pp. 2113–2117, 2020.
[7] S. K. Jain, "Review of Indian seismic code, IS 1893 (Part 1): 2002," *Indian Concrete Journal,* vol. 77, no. 11, pp. 1414–1422, 2003.
[8] C. P. Choudhury and J. Pathak, "Analytical study of seismic response of traditional Assam-type housing in north-east India," in *Proc. 15th Symposium on Earthquake Engineering IIT Roorkee*, 2014.
[9] NBC 105:1994 – Seismic Design of Buildings in Nepal, Department of Urban Development, Kathmandu.
[10] NBC 105:2020 – Seismic Design of Buildings in Nepal, Department of Urban Development and Building Construction, Kathmandu.
[11] IS 1893(Part I):2002 – Criteria for Earthquake Resistant Design of Structures, Part 1: General Provisions and Buildings, Bureau of Indian Standards, New Delhi.